[CANCER RESEARCH (SUPPL.) 50, 5658s–5667s, September 1, 1990]

# A Human Hepatocellular Carcinoma 3.0-Kilobase DNA Sequence Transforms Both Rat Liver Cells and NIH3T3 Fibroblasts and Encodes a 52-Kilodalton Protein[1, 2]

**Stringner Sue Yang,[3] Ke Zhang, Wilfred Vieira, Janet V. Taub, Jill H. Zeilstra-Ryalls, and Ronald L. Somerville**

*Laboratories of Cellular Oncology [S. S. Y., K. Z., J. V. T.] and Cell Biology [W. V.], National Cancer Institute, Bethesda, Maryland 20892, and Department of Biochemistry, Purdue University, West Lafayette, Indiana 47907 [J. H. Z-R., R. L. S.]*

## Abstract

**Neoplastic transformation of rat liver cells *in vitro* by DNA-mediated gene transfer with an oncogene, *hhc*$^M$, derived from human (Mahlavu) hepatocellular carcinoma, is described and compared with that of NIH3T3 cells. *hhc*$^M$ was cloned in a neomycin-resistant simian virus 40 promoter vector (pNeo$^r$/S) and was designated pN$^r$pM-1. BRL-1 or NIH3T3 cells, transfected with pN$^r$pM-1 DNA, showed significant morphological changes, loss of contact inhibition, and anchorage-independent growth. They became highly tumorigenic in nude rats and *nu/nu* mice. Control BRL-1 and NIH3T3 cells, whether transfected with pNeo$^r$/S DNA or not, remained contact inhibited and nontumorigenic. Both the transformants and the tumor cells contained integrated *hhc*$^M$ DNA as shown by Southern blot hybridization. The complete nucleotide sequence of the *hhc*$^M$ 3.0-kilobase DNA was also determined, and it consisted of a possible open reading frame for a protein of 52 kilodaltons (467 amino acids). The high-level production of a slightly modified form of this 52-kilodalton protein in a bacterial expression system has been successfully achieved. The bacteria-produced protein was similar in electrophoretic behavior to the 52- to 53-kilodalton protein synthesized in a cell-free translation system using rabbit reticulocyte lysate programmed with hybrid-selected *hhc*$^M$-specific mRNA from Mahlavu hepatocellular carcinoma cells.**

## Introduction

The DNA-mediated gene transfer technique on NIH3T3 cells *in vitro* has made it possible to identify certain tumor cellular DNA sequences with oncogenic potential that arose by point mutation(s) or rearrangement(s). Certain tumor-derived oncogenes were found to be homologous to viral oncogenes (1–5). The process of cell transformation is associated with the heightened expression of an oncogene or activated protooncogene, which may eventually lead to diverse phenotypic changes such as loss of contact inhibition, anchorage-independent growth, increase in cell refractility, morphological changes, tumorigenicity, elevated synthesis of certain proteins, and increased glucose uptake. The human *hhc*$^M$ oncogene is a 3.0-kilobase DNA fragment from the African Mahlavu hepatocellular carcinoma cells, and it was originally identified by its ability to transform NIH3T3 cells and was molecularly cloned in pUC 8 (6–8). With the use of *hhc*$^M$ DNA as a probe, a number of related sequences were demonstrated by Southern blot hybridization analysis in DNA samples prepared from 17 hepatocellular carcinomas of Asian origin (8). A few related clones have been isolated from the hepatoma DNAs, but only two of them showed cell-transforming capability (8).

Interest in *hhc*$^M$ became enhanced following the successful transformation of Buffalo rat liver (BRL-1) cells by transfection with *hhc*$^M$ DNA. Transformation of liver cells has been difficult to evaluate mainly because cultured liver cells, like BRL-1 (9), or short-term liver cell cultures usually constitute a mixed population of cells that include hepatocytes of epithelioid cells, glandular (acinar) cells, stromal cells, and interstitial cells. These cells undergo continuous, asynchronous biochemical differentiation. Morphological comparisons between control cells and transformants thus become difficult. *In vitro* transformation of the primary culture of differentiated rat hepatocytes following adenovirus infection and transfection with the adenovirus E1A and E1B DNA was reported earlier. The transfected cells became immortalized but were not tumorigenic in the neonatal syngeneic rat (10). Cultured rat hepatocytes transformed by virion or cloned SV40[4] DNA became tumorigenic at high passages (33 to 61) concomitant with enhanced expression of c-Ha-*ras*, suggesting a close relation between tumorigenicity and oncogene expression (11). Chemical hepatocarcinogenesis, both *in vivo* and *in vitro*, and the various molecular changes associated with the ensuing hepatomas have been well documented (12).

In this paper, we describe the transformation of BRL-1 cells by transfection with human *hhc*$^M$ DNA cloned in a construct that carries a neomycin resistance marker plus an SV40 promoter, pNeo$^r$/S (Fig. 2). Using neomycin resistance as a selectable marker, we were able to evaluate the effect and fate of the transfected human *hhc*$^M$ DNA in rat liver cells. Three plasmids, pN$^r$pM-1, pN$^r$pM-2, and pN$^r$M, carrying *hhc*$^M$ DNA in different orientations were constructed, and their transformation potency toward BRL-1 and NIH3T3 cells following DNA-mediated gene transfer was studied. The parameters used to evaluate cell transformation were morphological changes, the neomycin resistance phenotype, and anchorage-independent growth. The tumorigenicity of the transformed cells in Swiss-*nu/nu* mice and nude rats was also investigated.

The nucleotide sequence of the 3.0-kilobase *hhc*$^M$ DNA revealed an open reading frame, encoding a protein with a molecular weight of 52 kD. Here we present the nucleotide sequence of the *hhc*$^M$ DNA and describe the construction and expression in *Escherichia coli* of a chimeric form of the 52-kD *hhc*$^M$ polypeptide driven by the *lac* promoter.

## Materials and Methods

**Cells, Tissue Culture, DNA Transfection Assay, and Soft Agar Cloning of Transformed Cells.** NIH3T3 cells, passages 6 to 11, and BRL-1 cells for transfection assays were maintained in DMEM supplemented with 10% heat-inactivated fetal calf serum, penicillin (50 units ml$^{-1}$), and streptomycin (25 $\mu$g ml$^{-1}$) in a 5% $CO_2$ atmosphere at 37°C. BRL-1 is a liver cell line established earlier in serum-free medium conditioned

[1] Presented at the "XIVth Symposium of the International Association for Comparative Research on Leukemia and Related Diseases," October 8–12, 1989, Vail, CO.

This study was supported in part by a grant from the National Institute of General Medical Sciences (GM 22131) and by a contract from the National Cancer Institute (263-MD-929353) to R. L. S.

[2] *hhc*$^M$ ORF and p52 application: US Patent 07/451,953. Foreign Patent pending.

[3] To whom requests for reprints should be addressed, at EPN Room 308, National Cancer Institute, Bethesda, MD 20892.

[4] The abbreviations used are: SV40, simian virus 40; DMEM, Dulbecco's modified Eagle's medium; HMW, high molecular weight; poly A, polyadenylate; SSC, standard saline citrate; SDS, sodium dodecyl sulfate; ORF, open reading frame; kD, kilodalton.

by the cells, which produce a family of polypeptides termed multiplication-stimulating activity, which are considered to be related to somatomedins (9). All tissue culture materials were purchased from GIBCO, Long Island, NY.

DNA transfections were carried out by a modified calcium phosphate procedure for NIH3T3 cells as described earlier (6, 13). On Day 2 post transfection, gentamicin sulfate (G418) DMEM was added to the cells to enrich for cells expressing the *Neo*$^{r}$ gene. G418-resistant colonies were trypsinized and seeded at 150,000 cells/30-mm plate in 0.4% soft agar to test for colony formation capability. Colonies formed in soft agar were scored and expanded 3 wk later in G418-DMEM.

**Gentamicin Sulfate Dosimetry for BRL-1 Cells and the Effective pNeo$^{r}$ DNA Concentration for Transfection.** Differing from NIH3T3 cells, BRL-1 cells exhibit extreme sensitivity to gentamicin sulfate. To determine the appropriate concentration of G418, we carried out a survival study for BRL-1 cells, presented in Fig. 1*A*. The 100% lethal dose of G418 for control BRL-1 cells was found to be 0.15 to 0.2 mg ml$^{-1}$. The concentration against survival of BRL-1 cells can thus be achieved effectively at 0.25 mg ml$^{-1}$ of medium, whereas G418 selection against NIH3T3 cells, a well-documented phenomenon, required 0.5 mg ml$^{-1}$ of G418.

Similarly, by a pNeo$^{r}$ DNA concentration-dependent transfection assay, we found the optimal transfection dosage for BRL-1 cells to be 750 ng of pNeo$^{r}$ DNA (Fig. 1*B*). Transfection studies involving the three recombinant plasmids were thus carried out with molar equivalents of pNeo$^{r}$ DNA at 750 ng.

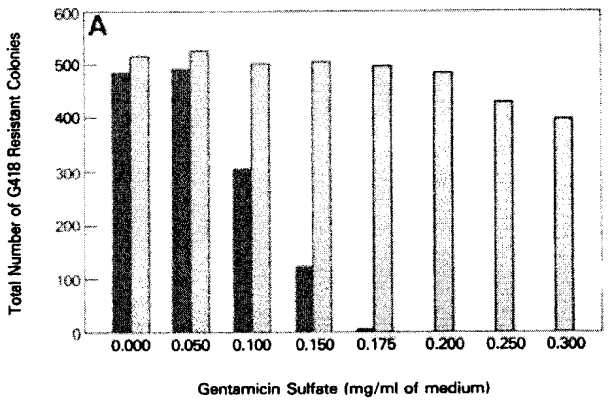


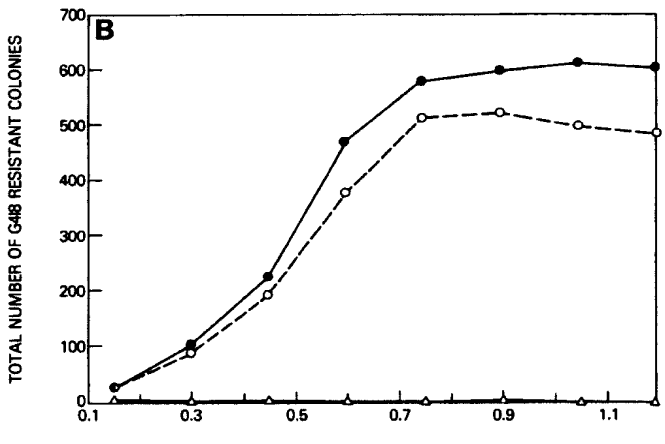


Fig. 1. *A*, dosimetry of gentamicin sulfate (G418), a synthetic neomycin analogue, in the selection of BRL-1 transfectants of pNeo$^{r}$/S DNA; *B*, effective dose of pNeo$^{r}$/S DNA for conferring neomycin resistance in G418 selection medium. In *A*, trypsinized BRL-1 cells were seeded at 300,000 cells per 30-mm tissue culture dish in the presence of specified concentrations of G418-supplemented DMEM. Survival of colonies was scored after control culture without G418 had reached confluence, usually within 12 to 18 days. *Solid bars* designate survival of control BRL-1 colonies. *Shaded bars* designate survival of transfectant colonies with 0.75 μg of pNeo$^{r}$/S DNA. In *B*, BRL-1 cells were transfected with the specified amount of pNeo$^{r}$/S DNA and seeded in duplicate dishes 24 h post transfection. G418 was introduced into the medium 48 h post transfection. Colony survival was scored on Day 21. All experimental details were as described in "Materials and Methods" (8). ●, NIH3T3 cells; ○, BRL-1 cells, both transfected with pNeo$^{r}$/S DNA. △, control NIH3T3 cells or BRL-1 cells transfected with carrier DNA (NIH3T3).

**Tumorigenesis.** Transformed cells from soft-agar colonies were expanded and inoculated s.c. at $10^{4}$ to $10^{6}$ cells in to Swiss-*nu/nu* mice. Tumorigenesis in the challenged mice was monitored closely. Pathological changes within organs and tissues were determined histologically.

**Preparation of DNA from Tissue Culture Cells and Tumors.** Total HMW DNA was extracted and purified from tissue culture cells and tumor tissues as described elsewhere (6, 14). The HMW DNA thus purified had been subjected to proteinase K digestion, with sequential chemical purification first with phenol-cresol, chloroform-isoamyl alcohol, ether, and ethanol-NaCl precipitation, followed by RNase digestion and a second sequential chemical purification. The purified DNA samples were dialyzed against Tris-EDTA-NaCl buffer (14) prior to use in transfection and other experiments.

**Plasmid Constructs and Plasmid DNA Preparation.** The constructs used in this study were prepared by ligation of the 3.0-kilobase *hhc*$^{M}$ DNA, as a *Hind*III fragment, to *Hind*III-cleaved pNeo$^{r}$/S vector. Cloning and screening procedures were as described elsewhere (14, 15). Three constructs were obtained, and restriction endonuclease cleavage patterns for these three constructs verified their correctness.

Plasmid DNA was prepared by the rapid heating method, followed by isopyknic centrifugation at 180,000 × *g* for 20 h in cesium chloride-ethidium bromide (14, 15). Samples of banded plasmid DNA were dialyzed against Tris-EDTA-NaCl buffer prior to use in transfection and other experiments.

**Preparation of [$^{32}$P] Nick-translated *hhc*$^{M}$ DNA.** Purified *hhc*$^{M}$ 3.0-kilobase DNA was nick-translated as described (14, 15). All deoxynucleoside [$^{32}$P]triphosphates (specific activity, 3000 Ci mM$^{-1}$) were purchased from Amersham, Arlington Heights, IL. DNA polymerase I, Klenow fragment, T4 polynucleotide kinase, and T4 DNA polymerase were purchased from New England Biolabs, Beverly, MA; International Biotechnology Institute, New Haven, CT; or Bethesda Research Laboratory, Rockville, MD. All other chemicals, unless specified, were purchased from Sigma Chemical Co., St. Louis, MO. Random primers were also used in the preparation of certain radioactive endonuclease restricted DNA fragments.

**DNA-DNA Hybridization Analysis.** HMW DNA samples purified from various transfected BRL-1 or NIH3T3 cells and tumors were digested with a suitable restriction endonuclease, subjected to electrophoresis in 0.8% or 1.0% agarose gel, transferred onto nitrocellulose filters, and hybridized against a specific [$^{32}$P]DNA probe at $10^{6}$ cpm ml$^{-1}$. The conditions of hybridization, stringency, and stripping of bound radioactivity from the filter were as previously described (8).

**Messenger RNA Preparation and Cell-free Translation of Hybrid-selected *hhc*$^{M}$-specific mRNA.** The preparation of poly A-rich RNA and cell-free translation of the hybrid-selected *hhc*$^{M}$-specific mRNA were carried out as described earlier (15). Poly A-rich RNA was separated from total RNA of log-phase cells (Mahlavu hepatocellular carcinoma and *hhc*$^{M}$ DNA-transformed NIH3T3 tumor 8/1E) by oligo dT-cellulose column chromatography. Poly A-rich RNA was then allowed to anneal for 20 h to 5 μg of *hhc*$^{M}$ DNA impregnated on S & S nitrocellulose filters under optimal conditions for DNA-RNA hybridization. The filter was washed free of unbound RNA, and the annealed mRNA was released by heating to 80°in 0.1× SSC. This *hhc*$^{M}$-specific mRNA was used to program cell-free protein synthesis in a rabbit reticulocyte lysate system with [$^{35}$S]methionine as label (New England Nuclear, Boston, MA). The resulting $^{35}$S-labeled polypeptides were separated by SDS-polyacrylamide gel electrophoresis and detected by autoradiography.

**DNA Sequencing.** A series of overlapping clones was generated using available restriction sites and a modification of the primer extension method of McKnight and Kingsbury (16) with synthetic oligodeoxynucleotide (20 to 22 nucleotides long) complementary to the *hhc*$^{M}$

DNA. Both the positive and negative strands of *hhc*$^{M}$ DNA were completely sequenced. Nucleotide and amino acid sequences were analyzed with computer programs from the Bionet System and Genbank.

## Results

**Constructs Containing *hhc*$^{M}$ DNA and Transformation of Buffalo Rat Liver Cells Compared with NIH3T3 Cells.** Fig. 2 depicts the three constructs carrying *hhc*$^{M}$ 3.0-kilobase DNA in different orientations as verified by restriction endonuclease cleavage analysis. Clone pN$^{r}$M (8.9 kilobases) carried *hhc*$^{M}$ DNA ligated to the pNeo$^{r}$/S 5.8-kilobase DNA so that the 5′ terminus of *hhc*$^{M}$ DNA was situated at the 3′ end of the *Neo*$^{r}$ locus of the pNeo$^{r}$/S DNA in a 5′ to 3′ direction. Clones pN$^{r}$pM-1 and pN$^{r}$pM-2 (11.6 kilobases each) retained the pUC 8 sequence of the original clone of *hhc*$^{M}$, PM-1 (7, 8). The two clones differed in orientation with respect to the relation between the termini of *hhc*$^{M}$ DNA and the promoter sequence of SV40 or the Neo$^{r}$ sequence. Upon transfections of these DNA samples into BRL-1 cells or NIH3T3 cells, all the transformants showed an initial active expression of the *pNeo*$^{r}$ gene and survived G418 selection at the respective effective concentration that was lethal to the control untreated BRL-1 cells (Fig. 1*A* and Fig. 3*a*) or NIH3T3 cells (Fig. 3*a*). Fig. 3 shows a typical experiment in which the neomycin resistance was conferred by transfection with all three constructs, pN$^{r}$pM-1, pN$^{r}$pM-2, and pN$^{r}$M, to BRL-1 cells. BRL-1 cells transformed by pN$^{r}$pM-1 DNA were found to tolerate G418 concentrations beyond 0.3-mg ml$^{-1}$ (Fig. 1) and even as high as 0.40 mg ml$^{-1}$ of medium (data not shown). This method yielded $10^{3}$ colonies $\mu g^{-1}$ of input DNA in transfection experiments with clones pN$^{r}$pM-1, pN$^{r}$pM-2, and pN$^{r}$M. The assay can be scored within 12 to 14 days post transfection.

**Stability of Neomycin Resistance and Transformed Phenotypes through Secondary and Tertiary Transfection and in Progeny Tumor Cells.** The stability studies on neomycin resistance, anchorage-independent growth, and tumorigenicity through two subsequent transfection cycles and in progeny tumor cells are summarized in Table 1. Although all selected colonies initially expressed the neomycin resistance phenotype (Fig. 3), this characteristic was not stably transmitted in either the pN$^{r}$M or pN$^{r}$pM-2 transformant on passage through *nu/nu* mice (Table 1). One construct, pN$^{r}$pM-1, was extremely stable through secondary and tertiary transfections and repeated challenges in *nu/nu* mice. For that reason, studies on BRL-1 cells were primarily carried out with the pN$^{r}$pM-1 clone.

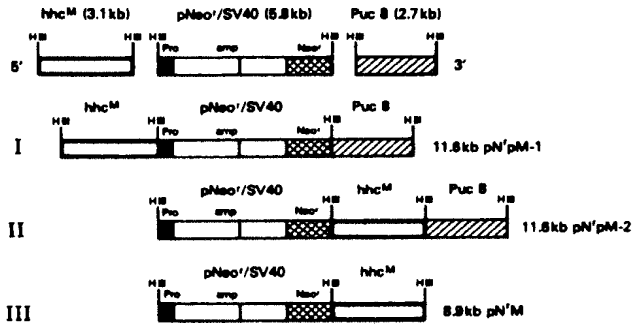


Fig. 2. Constructs carrying the human *hhc*$^{M}$ 3.0- to 3.1-kilobase DNA in a neomycin resistance vector. The original clone of *hhc*$^{M}$, PM-1 (8), was digested with *Hind*III restriction endonuclease to release both the *hhc*$^{M}$ DNA and pUC 8 (2.7 kilobases) DNA. These fragments were ligated to the *Hind*III-cleaved DNA of the pNeo$^{r}$/S vector. DNA concentrations for ligation were at a ratio of 1:1:2 with respect to *hhc*$^{M}$ DNA:pUC 8 DNA:pNeo$^{r}$/S DNA. The resultant clones were designated pN$^{r}$pM-1, 11.6 kilobases (*I*), pN$^{r}$pM-2, 11.6 kilobases (*II*), and pN$^{r}$pM, 8.9 kilobases (*III*). *Pro*, SV40 promoter; *amp*, ampicillin resistance locus; *Neo*$^{r}$, neomycin resistance locus; *kb*, kilobase(s); *H III*, *Hind*III.

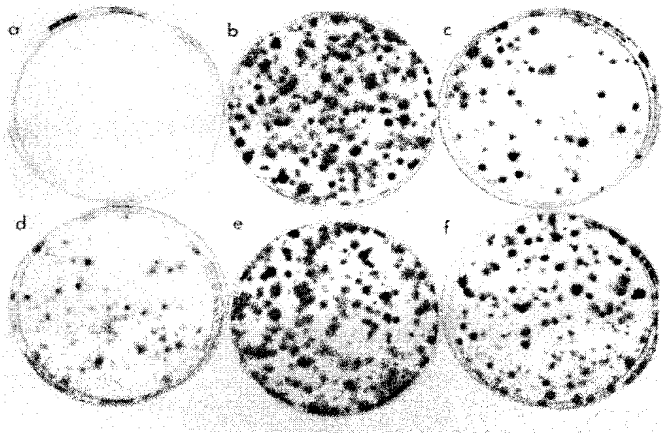


Fig. 3. Neomycin-resistant colonies of BRL-1 cells transfected by the DNAs prepared from pN$^{r}$pM-1, pN$^{r}$pM-2, and pN$^{r}$pM clones. *a*, no surviving control BRL-1 or NIH3T3 cells in G418 selection medium. The G418 selection dosage for transfected BRL-1 cells was 0.25 mg ml$^{-1}$ of medium in *a*, *b*, *c*, *d*, and *f*. The G418 selection dosage for pN$^{r}$pM-1-transformed NIH3T3 cells was 0.50 mg ml$^{-1}$ of medium in *a* and *e*. The surviving colonies of BRL-1 cells were transfected with pN$^{r}$pM-1 DNA (*b*), pN$^{r}$pM-2 DNA (*c*), pN$^{r}$pM DNA (*d*), and pNeo$^{r}$/S DNA (*f*). The surviving colonies of NIH3T3 cells were transfected with pN$^{r}$pM-1 DNA (*e*). The DNA dosage used in transfection was 750 ng for pNeo$^{r}$/S, 1125 ng for pN$^{r}$pM, and 1500 ng each for pN$^{r}$pM-1 and pN$^{r}$pM-2.

Secondary transfection of both BRL-1 cells and NIH3T3 cells with total genomic DNA purified from the primary pN$^{r}$pM-1 transformants resulted in successful transmission of both the cell transformation property as well as the G418 resistance phenotype (Table 1). Successful transmission of both the transformed morphology as well as the G418 resistance to the recipient NIH3T3 cells was also achieved with the secondary NIH3T3 transformant DNA in a tertiary transfection, suggesting that the transfected DNA had become stably integrated.

**Morphological Changes, Anchorage-independent Growth, and Tumorigenesis of BRL-1 and NIH3T3 Transformants Transfected with the *hhc*$^{M}$-pNeo$^{r}$/S Constructs.** Varying degrees of transformed morphology, *i.e.*, round and spindle-shaped and highly refractile cells, were associated with different cultures of either BRL-1 (Fig. 4, ii and iii) or NIH3T3 (Fig. 5*B*, ii and iii) cells transfected with pN$^{r}$pM-1 DNA. Control BRL-1 and NIH3T3 (Fig. 5*A*i) cultures generally appeared flat and contact inhibited. When transfected with pNeo$^{r}$/S DNA, both types of cultures showed some scattered round and refractile cells, but they retained contact inhibition (Figs. 4i and 5*B*i). Transformation of NIH3T3 cells by *hhc*$^{M}$ DNA carried in the pUC 8 plasmid has already been described (Fig. 5*A*ii) (8). NIH3T3 cells, transfected with pN$^{r}$pM-1, pN$^{r}$pM-2, or pN$^{r}$M DNA, showed a significant increase in growth density, a loss of contact inhibition, and an increase in cell refractility. A typical focal transformation of NIH3T3 cells transfected with pN$^{r}$pM-1 DNA at 12 days post transfection (Fig. 5*B*ii) and 18 days post transfection (Fig. 5*B*iii) is shown in Fig. 5. Transformation of heterogeneous liver cell populations with pN$^{r}$pM-1 DNA, however, was limited to certain types among the hepatocytes. They appeared round, highly refractile, and clustered in high cell density (Fig. 4ii at 14 days post transfection and 4iii at 21 days post transfection); they also showed a tendency to detach from the culture. Cytoplasmic secretory vacuoles developed within transformed BRL-1 cells, and secretory material was released into the culture medium as mucinous materials tightly associated with the cell surface. Surrounding these apparently trans-

Table 1 *Persistence of neomycin resistance, anchorage-independent growth, and tumorigenicity through three transfection cycles*
For each study, all experimental detail was as described in "Materials and Methods."

| | G418 resistance | | Anchorage-independent growth | | Tumorigenicity | |
|---|---|---|---|---|---|---|
| | BRL-1 | NIH3T3 | BRL-1 | NIH3T3 | BRL-1 | NIH3T3 |
| pN$^{r}$pM-1 DNA-transfected cells | | | | | | |
| Primary transformant | + | + | + | + | + | + |
| Soft agar colony clone | + | + | + | + | + | + |
| Primary tumor cells in tissue culture | + | + | + | + | | |
| Secondary transfectant | + | + | + | + | + | + |
| Secondary tumor cells in tissue culture | + | + | + | + | ND[a] | + |
| Tertiary transfectant | ND | + | ND | + | ND | + |
| Tertiary tumor cells in tissue culture | ND | + | ND | + | | |
| pN$^{r}$M DNA-transfected cells | | | | | | |
| Primary transformant | + | + | − | − | − | +[b] |
| Soft agar colony clone | NT | − | | | | |
| Primary tumor cells in tissue culture | NT | −[b] | | | | |
| pN$^{r}$pM-2 DNA-transfected cells | | | | | | |
| Primary transformant | + | + | − | − | − | +[b] |
| Soft agar colony clone | NT | NT | | | | |
| Primary tumor cells in tissue culture | NT | −[b] | | | | |

[a] ND, not yet determined; NT, not tested because of inability to test the cells due to negative findings.
[b] Tumor nodule developed at site of inoculum 5 to 6 mo post challenge.

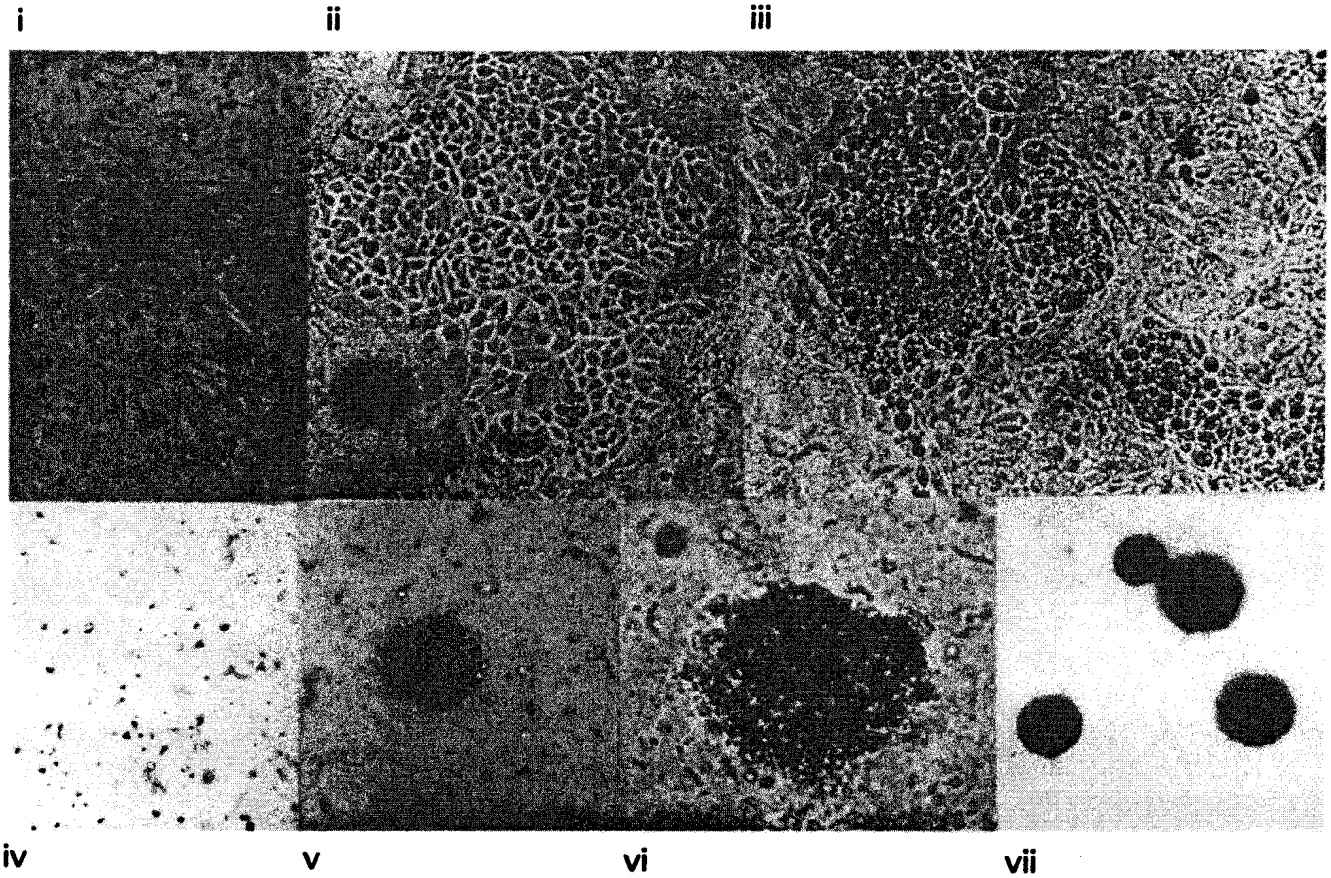


Fig. 4. Morphological changes and anchorage-independent growth of Buffalo rat liver (BRL-1) cells post transfection with human *hhc*$^{M}$ DNA carried in a construct, pN$^{r}$pM-1. Neomycin-resistant colonies of BRL-1 cells transfected with pNeo$^{r}$/S DNA, 750 ng (*i*), and transformed foci of BRL-1 culture at 14 days (*ii*) and at 21 days (*iii*) post transfection with pN$^{r}$pM-1 DNA (1.5 μg), showing progressive increase in refractility and loss of contact inhibition. Anchorage-independent growth exhibited by pNeo$^{r}$/S DNA-transfected BRL-1 cells (*iv*) from culture at *i* showing no soft agar colony formation (× 20). Soft agar colonies of pN$^{r}$pM-1-transformed BRL-1 cells from culture at *iii* are shown at magnifications of × 20 (*v*) and × 200 (*vi*), phase-contrast microscopy; (*vii*), the same at × 200, light microscopy. Details for the transfection assay and for colony formation in soft agar were as described in "Materials and Methods."

formed foci are other epithelioid cells that seemed to remain contact inhibited. BRL-1 transformants with pN$^{r}$pM-1 DNA, expanded from the transformed focus, exhibit a growth density 6- to 8-fold greater than that of the control BRL-1 cells with or without pNeo$^{r}$/S DNA transfection (Fig. 6).

To further confirm that *hhc*$^{M}$ DNA actually conferred the

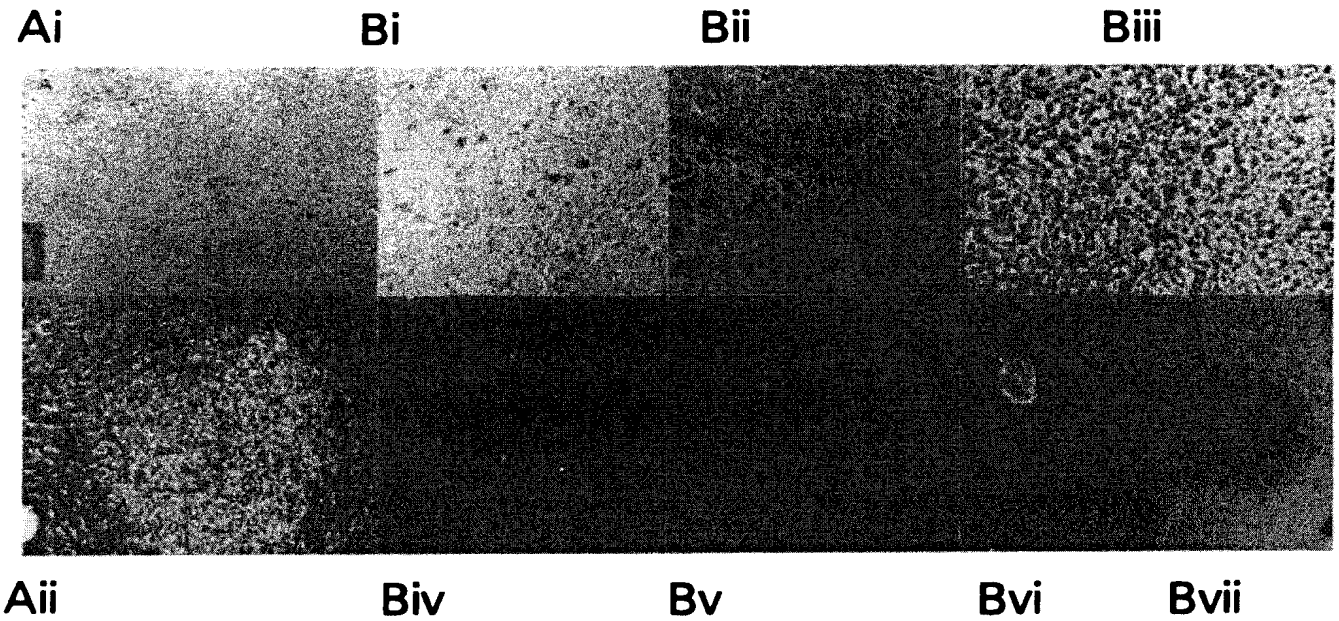


Fig. 5. Morphological changes and anchorage-independent growth of NIH3T3 cells transformed with *hhc*$^{M}$ DNA. *Ai*, control NIH3T3 culture, transfected with carrier NIH3T3 DNA, 28 days posttransfection (× 80). *Aii*, a transformed focus of NIH3T3 cells transfected with *hhc*$^{M}$ DNA carried in pUC 8 plasmid, 1.0 μg/plate, 28 days post transfection (× 180, phase-contrast microscopy). *Insets* in *Ai* shows that no tumor developed in a Swiss-*nu/nu* mouse given an injection of $10^6$ control transfected cells from *Ai* culture, 47th week post injection. *Inset* in *Aii* shows an NIH Swiss-*nu/nu* mouse inoculated with $10^6$ NIH3T3 transformants from *Aii*, bearing tumor 16 wk post injection. *Bi*, G418-resistant colonies of NIH3T3 cells transfected with pNeo$^r$/S DNA; *Bii and Biii*, with pN$^r$pM-1 DNA (1.25 μg each). No soft agar colony formation by NIH3T3 transfectants with pNeo$^r$ DNA (*Biv*) was observed. Soft agar colony formation was observed by NIH3T3 transformants with pN$^r$pM-1 DNA. (× 20, *Bv*; × 200, *Bvi*, phase-contrast microscopy) and by tumor cells of pN$^r$pM-1 DNA NIH3T3 transformants (× 200, light microscopy; *Bvii*).

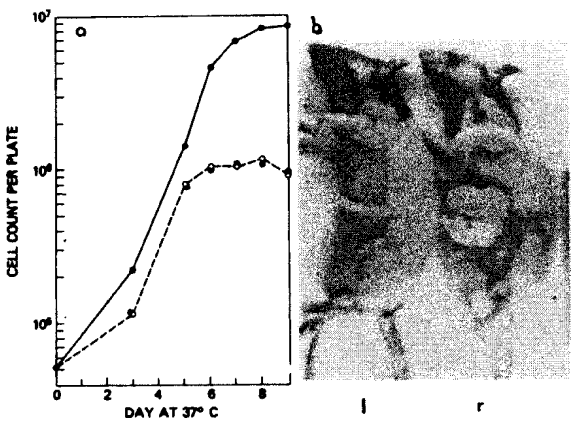


Fig. 6. *A*, growth density and tumorigenicity of transformed BRL-1 soft agar clone 4 cells as compared with control pNeo$^r$/S DNA-transfeceted BRL-1 cells. Transformed BRL-1 soft agar clone 4 cells (●), previously expanded in tissue culture; cells of pNeo$^r$/S DNA-transfected culture (○) and control BRL-1 cells (◑) were seeded at 50,000 cells per 100-mm plate. Growth was monitored by viable cell counts stained with trypan blue. *b*, tumorigenesis of clone 4 BRL-1 transformant with pN$^r$pM-1 DNA in the nude rat. Nude rats were given injections homotropically with $10^6$ cells from a clone 4 BRL-1 transformant with pN$^r$pM-1 DNA, a transfectant of pNeo$^r$/S DNA, or none. At *left* (*l*), no tumor developed with rats receiving only BRL-1 cells or BRL-1 transfectant of pNeo$^r$/S DNA 5 mo post injection. At right (*r*), a nodule developed in a rat inoculated with clone 4 transformed BRL-1 cells by 6 wk post injection; rat on right, 11 wk post injection.

transformed phenotype, pN$^r$pM-1 transformants were seeded in soft agar to score anchorage independence. Control NIH3T3 and BRL-1 cells, with or without pNeo$^r$/S DNA transfection, failed to form colonies in soft agar (Figs. 4iv and 5*B*iv). Individual cells from transformed foci of BRL-1 and of NIH3T3 cells that had taken up pN$^r$pM-1 DNA, when cloned and expanded in G418 selection medium formed colonies in soft agar (Figs. 4, v to vii, and 5*B* v and vi).

BRL-1 or NIH3T3 cells that had been transformed with pN$^r$M or pN$^r$pM-2 DNA failed to form soft agar colonies within the time frame comparable to that of the other transformants (data not shown). However, both types of NIH3T3 transformants were tumorigenic in Swiss-*nu/nu* mice, although longer latency periods were observed (Table 1). The ability to form colonies in soft agar probably depends on the ability of transformed cells to replicate in an anaerobic environment. Clones pN$^r$pM-1 and pN$^r$pM-2 differ from one another in the orientation of the *hhc*$^{M}$ sequence with respect to the SV40 promoter sequence (Fig. 2). However, there is no direct evidence that this orientation difference affects the ability of pN$^r$pM-2 transformants to form colonies in soft agar.

BRL-1 and NIH3T3 transformants of pN$^r$pM-1 DNA expanded from the soft agar colonies proved to be highly tumorigenic when inoculated s.c. into Swiss-*nu/nu* mice at $10^5$ or $10^6$ cells (Table 1). The same results were obtained with BRL-1 transformants in nude rats at $10^6$ cells (Fig. 6b). Tumors developed within 6 to 20 wk post inoculation. Control cells, either NIH3T3 or BRL-1, with or without pNeo$^r$/S DNA transfection, failed to develop tumors or other forms of neoplasms at the same challenge dose (Figs. 5*A*i, *inset*, and 6*b*) even at 12 mo post inoculation. Of the 72 Swiss-*nu/nu* mice challenged with NIH3T3 transformants, over 85% developed tumors within 3 mo. Among the tumor-bearing *nu/nu* mice, 20% also developed lymphoadenopathy, splenomegaly, and lymphoma. Five % of the mice inoculated with $10^5$ transformed cells developed tumors after 5 to 6 mo. Five % of the animals developed ascites in addition to lymphoadenopathy and splenomegaly. The residual 5% of the challenged mice failed to show any tumor. It appears certain that the *hhc*$^{M}$ DNA carried in either pUC 8 or

the pNeo$^r$/S vector bestowed the tumorigenic potential upon transfection into both NIH3T3 and BRL-1 cells. The multipotential nature of the oncogenic mechanism remains to be explored.

Cells expanded from tumors of either BRL-1 or NIH3T3 transformants formed large colonies in soft agar efficiently within 14 to 28 days (Figs. 4vii and 5*B*vii). Furthermore, cells expanded from these soft agar colonies showed a much shorter latency period and increased significantly in tumorigenic potential, such that rechallenge experiments on *nu/nu* mice or nude rats required greatly reduced doses (*e.g.*, $<10^2$ cells).

***hhc*$^M$ and pNeo$^r$/S Sequences in Tumors of NIH3T3 and BRL-1 Cells Transformed with pN$^r$pM-1 DNA.** The presence of the human DNA sequence in transformed cells was demonstrated by Southern blot hybridization with genomic DNAs of tumors that developed from NIH3T3 and BRL-1 cell transformants using a nick-translated [$^{32}$P]-*hhc*$^M$ DNA probe (Fig. 7). Among the primary tumor DNA samples, the *hhc*$^M$-specific sequence was demonstrated in *Lane NT* for tumor of NIH3T3 transformants and in *Lane BRLT* for BRL-1 transformants. Similarly, using a $^{32}$P-pNeo$^r$/S DNA probe, the pNeo$^r$ sequence was identified in the same tumor DNAs (*Lanes NT* and *BRLT*) as well as in DNAs from control NIH3T3 and BRL-1 cells transfected with pNeo$^r$/S DNA (*Lanes pN$^r$N* and *pN$^r$BRL*). Control NIH3T3 and BRL-1 DNAs were totally negative. It is evident that the human *hhc*$^M$ DNA was integrated into both NIH3T3 and BRL-1 transformants and their respective tumors and was transmitted stably into progeny. Transformation of BRL-1 and NIH3T3 cells is thus mediated through transfection with pN$^r$pM-1 DNA bearing a human hepatoma DNA sequence, *hhc*$^M$, with transforming potential not only for NIH3T3 fibroblasts but also for rat liver cells.

**The Complete Nucleotide Sequence of *hhc*$^M$.** Since the restriction endonuclease cleavage map for *hhc*$^M$ 3.0-kilobase DNA has been described earlier (8), appropriate restriction sites were used for establishing M13 subclones for nucleotide sequencing (Fig. 8*A*). In addition, in order to elucidate both strands of the *hhc*$^M$ 3.0-kilobase DNA a modification of the McKnight and Kingsbury protocol (16) was used. Altogether it involved construction of 12 overlapping M13 subclones carrying inserts of the *hhc*$^M$ DNA fragments in both orientations (Fig. 8*A*). Where there was no convenient restriction endonuclease cleavage site, a primer extension method was used. Synthetic oligodeoxynucleotides (20 to 22 nucleotides) complementary to *hhc*$^M$ DNA were used as sequencing primers.

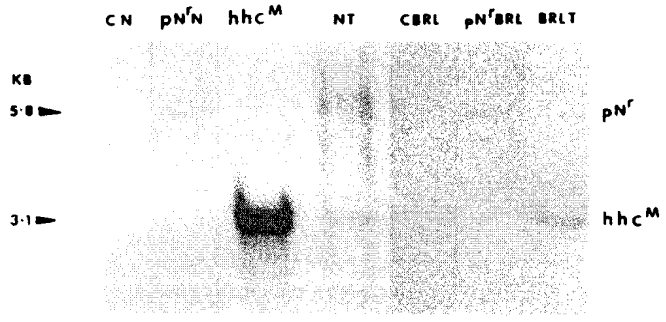


Fig. 7. Human DNA sequences in genomic DNAs prepared from tumors of NIH3T3 and BRL-1 cells transformed by pN$^r$pM-1 DNA. Sequential Southern blot hybridization of *Hind*III-digested tumor DNA or transfected cell DNA (50 $\mu$g/sample) were carried out first using a [$^{32}$P]-*hhc*$^M$ probe (3.0-kilobase DNA fragment) and then against a [$^{32}$P]-pNeo$^r$/S probe (5.8-kilobase DNA fragment). *Lanes CN* and *pN$^r$N* designate cellular DNAs from NIH3T3 cells transfected with c-*hhc* DNA, a human liver homologue (8), and pNeo$^r$/S DNA, respectively. Since no tumor developed from the challenged mice, DNA was prepared from the inoculum cells. *Lane hhc*$^M$ (0.1 $\mu$g) is the human hepatoma 3.1-kilobase DNA, a positive hybridization control. *Lane NT* is DNA from a tumor developed in a *nu/nu* mouse challenged with transformed NIH3T3 cells transfected with pN$^r$pM-1 DNA. *Lanes CBRL, pN$^r$BRL*, and *BRLT* designate DNA samples from control BRL-1 cells, BRL-1 cells transfected with pNeo$^r$/S DNA and from a tumor of BRL-1 transformants (soft agar clone 4 transfected with pN$^r$pM-1 DNA), respectively. All experimental details are as described in "Materials and Methods."

The complete nucleotide sequence for *hhc*$^M$ DNA is presented in Fig. 8*B*. The most prominent structural feature within this sequence is an open reading frame of 1401 nucleotides, potentially encoding a protein of 467 amino acids (52 kD). No significant homology was detected between the structure predicted by the open reading frame within *hhc*$^M$ with any other oncogene product or cellular protein. The protein-coding sequence was preceded and followed by punctuation elements appropriate to eukaryotic cells (such as the *TA TAA box*, AGGA ribosomal RNA binding site, and ATG start codon), suggesting that it might be efficiently expressed in hepatoma cells.

A possible second ORF of 591 nucleotides downstream of the p52 sequence was terminated by a TGA stop codon. This putative polypeptide was found to share partial homology with known protein sequences, probably because of the presence of a repetitive sequence in this area. These observations suggest that that *hhc*$^M$ DNA sequence might be the product of a DNA rearrangement involving a sequence of relatively significant size.

***hhc*$^M$ p52 Is Actively Expressed in Mahlavu Hepatocellular Carcinoma and NIH3T3 Transformants.** Using immobilized *hhc*$^M$ DNA, the *hhc*$^M$-specific messenger RNA was hybrid-selected from poly A-rich RNA preparations derived from Mahlavu hepatocellular carcinoma cells and from a tumor (8/1E) of transformed NIH3T3 cells (6, 7). Fig. 9*A* shows a 1.8-kilobase mRNA species identified by Northern blot hybridization in the poly A RNA purified from 8/1E tumor and a much larger $\geq$9.4-kilobase species of mRNA in the poly A RNA purified from Mahlavu hepatocellular carcinoma. No *hhc*$^M$-hybridizable RNA could be identified in RNA preparations from normal liver or control NIH3T3 cells transfected with a normal liver homologue c-*hhc* (8) (data not shown). Using hybrid-selected, *hhc*$^M$-specific mRNAs to program cell-free translation with [$^{35}$S]methionine and rabbit reticulocyte lysates, the major product visualized following autoradiography was a protein of about 52 to 53 kD, specified by the 1.8-kilobase 8/1E tumor mRNA [Fig. 9*B*, *Lanes N(hhc*$^M$*)*, 0.5 $\mu$g and 3.0 $\mu$g]. On the other hand, the large ($\geq$9.4 kilobase) mRNA hybrid-selected from Mahlavu hepatocellular carcinoma specified proteins of 52 to 53 kD, 42 kD, 32 kD, 24 kD, and 45 kD (trace) (Fig. 9*B*, *Lanes MAH*, 0.5 $\mu$g and 3.0 $\mu$g). No *hhc*$^M$-specific protein bands were identified in samples using normal liver and control N(c-*hhc*) poly A RNAs hybrid-selected with *hhc*$^M$ DNA [Fig. 9, *Lanes* N(c-*hhc*), 3 $\mu$g and liver, 0.5 and 3.0 $\mu$g]. This was probably because of the fact that the expression of a sequence related to *hhc*$^M$, c-*hhc*, in c-*hhc*-transfected NIH3T3 cells or normal liver was at a minimal level and, hence, no RNA was hybrid-selected hy *hhc*$^M$ DNA.

From the Northern blot analysis of *hhc*$^M$-specific mRNA identified in the 8/1E tumor and the size of the ORF in *hhc*$^M$ DNA, the 52- to 53-kD protein is considered most likely the oncoprotein specified by the ORF within *hhc*$^M$ DNA. The relative abundance of the *hhc*$^M$-specific mRNA also suggests that it is actively expressed by both the 8/1E tumor and especially the Mahlavu hepatocellular carcinoma cells.

**High Level Expression of the 52-kD *hhc*$^M$ Protein by *E. coli*.** The *hhc*$^M$ nucleotide sequence contains an ORF of 467 codons potentially encoding a protein of approximately 52 kD. This

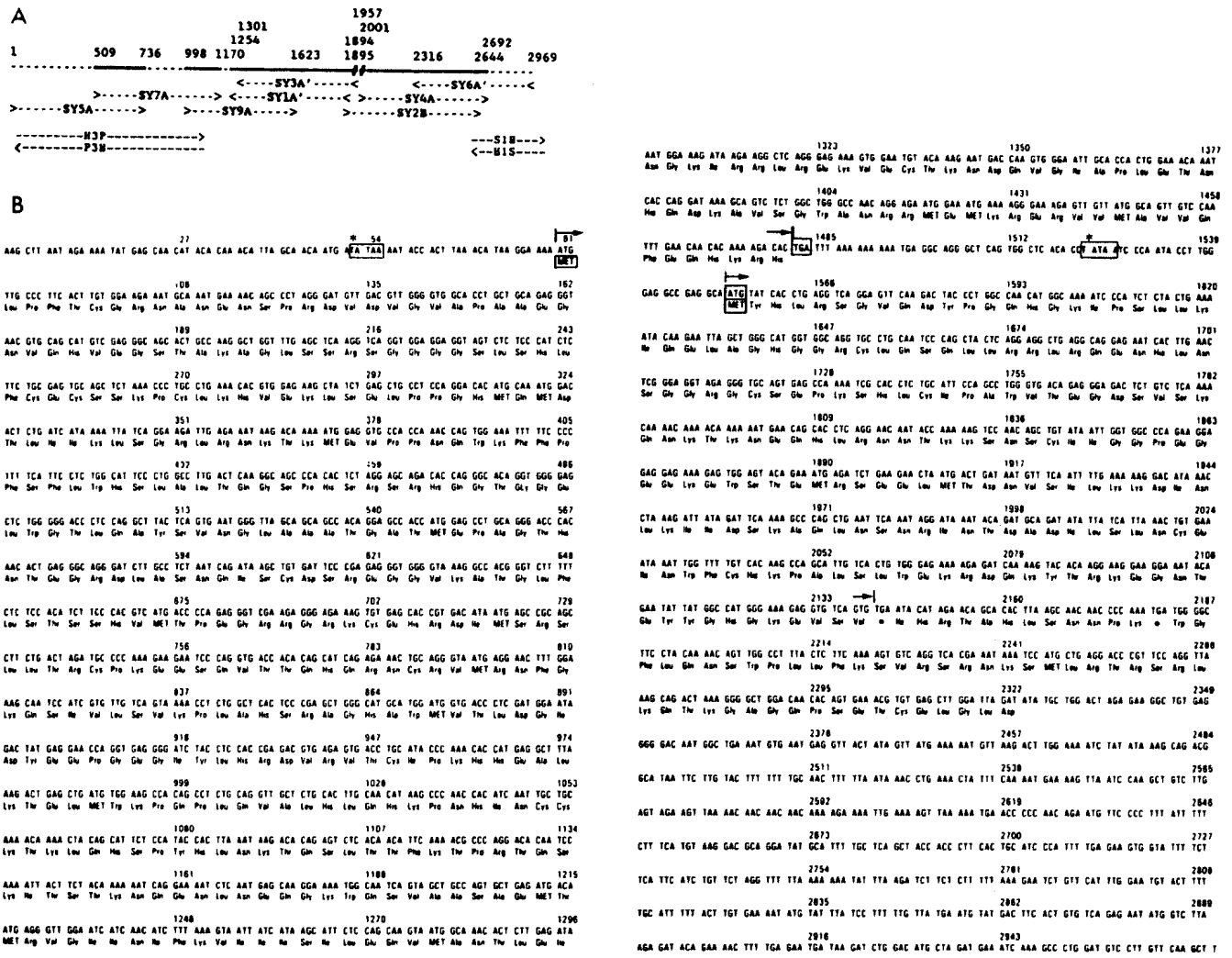

**Fig. 8.** *A*, sequencing strategy for *hhc*$^{M}$ 3.0-kilobase DNA. Twelve subclones were constructed. The *SY* series were M13 subclones analyzed by the Sanger dideoxy sequencing method. The subclones at the 5′ and 3′ termini, *H3P*, *P3H*, *SIH*, and *HIS*, were used for the Maxam-Gilbert sequencing method (17). *B*, complete nucleotide sequence of the human 3.0-kilobase *hhc*$^{M}$ DNA from Mahlavu hepatocellular carcinoma.

ORF resides at the 5′ half of the *hhc*$^{M}$ sequence (Fig. 8*B*). It is preceded by an appropriate ribosome recognition sequence (AGGA) and a TATAA box. A potential eukaryotic RNA polymerase II enhancer sequence (ATGCAAAT) is situated within 30 nucleotides of the start codon (ATG) at coordinate 79. The 52-kD protein detected in cell-free translation experiments with hybrid-selected *hhc*$^{M}$-specific mRNA (Fig. 9*B*) may thus be a possible product of the 467-codon ORF.

The protein-coding capability of this ORF was tested by juxtaposing this nucleotide sequence to a functional prokaryotic punctuation element. Fig. 10 depicts the construction of an expression plasmid (pJZ102) in which 18 codons from the 5′ terminus of the presumptive *hhc*$^{M}$ ORF were replaced by 11 amino acids of *lacZ*. This operation permitted the expression of *hhc*$^{M}$ ORF in the form of a chimeric protein, driven by the *lac* promoter.

*E. coli* cells transformed by pJZ102 were grown in rich medium to log phase and then induced with IPTG, whereupon high-level production of the chimeric *hhc*$^{M}$-*lac* fusion protein was observed (Fig. 11*a*). Kinetic analysis of the proteins encoded by pJZ102 showed increasing accumulation of a 52-kD protein over time. Production was maintained at high levels for 20 h (Figs. 11, *Lanes e* to *g*, and 12 *A*, *Lanes c* to *e*). The chimeric protein accumulated in bacterial cells as inclusion bodies, thus facilitating microscopic monitoring of the expression of p52 (compare Fig. 11, *Lanes a′*, *d′*, *e′*, *f′*, and *g′*). A control construct, pJZ101 (Fig. 10), in which the *hhc*$^{M}$-*lac* chimeric gene was interrupted by a Kanamycin cassette, failed to produce the 52-kD protein but synthesized instead the 28-kD aminoglycoside phosphotransferase (Fig. 12*A*, *Lane f*).

The large-scale bacterial production of the 52-kD *hhc*$^{M}$ protein laid the groundwork for the partial purification of this protein by SDS-polyacrylamide gel electrophoresis to homogeneity. The gel-purified p52 (Fig. 12*A*, *Lanes a* and *b*) was used to generate rabbit polyclonal antibodies. Sera from immunized animals displayed reactivity toward detergent-solubilized cell extracts from human hepatomas including Mahlavu and HPG2, pN′pM-1-transfected BRL-1 tumor cells, and purified p52, but not with extracts of BRL-1 cells (Fig. 12*B*). Cross-reactivity between polyclonal anti-p52 and solubilized extracts from Hp3P21.7 was barely detectable.

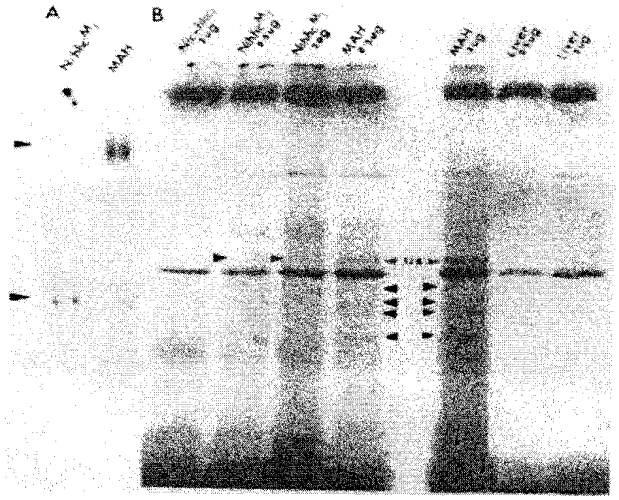

Fig. 9. *hhc*$^{M}$-specific mRNA species demonstrated by Northern blot hybridization and *hhc*$^{M}$-specific mRNA-directed cell-free protein synthesis. *A*, Northern blot hybridization with poly A RNA prepared from the *hhc*$^{M}$-transformed NIH3T3 tumor (8/1E) cells [*N*(*hhc*$^{M}$)], showing a 1.8-kilobase mRNA species and a ≥9.4-kilobase mRNA species from Mahlavu hepatocellular carcinoma (*MAH*) using a $^{32}$P-*hhc*$^{M}$ 3.1-kilobase DNA probe; none was identified in normal liver RNA (data not shown). Samples of 5 μg of poly A RNA were subjected to the routine formaldehyde gel electrophoresis, electrotransferred, and then subjected to hybridization as described earlier (14, 15). *B*, cell-free translation of hybrid-selected mRNAs from the same sources including *N*(*hhc*$^{M}$) and *MAH* and from *liver* and *N*(*c-hhc*), NIH3T3 cells transfected with a liver homologue c-*hhc*. mRNA concentrations used were 0.5 μg and 3 μg for each type. *hhc*$^{M}$ 3.0-kilobase DNA, 1 μg each, was impregnated in nitrocellulose filters, denatured, and subjected to hybridization with the specified poly A RNA sample. The filter was washed repeatedly and the hybridized RNA was released by heating to 80°C for 1 min in 0.1× SSC. The released *hhc*$^{M}$-specific mRNA samples were then used to program cell-free translation in a rabbit reticuloyte lysate system (New England Nuclear) using [$^{35}$C]methionine as label. All experimental detail has been described in "Materials and Methods" (14, 15) and in the technical manual provided by NEN.

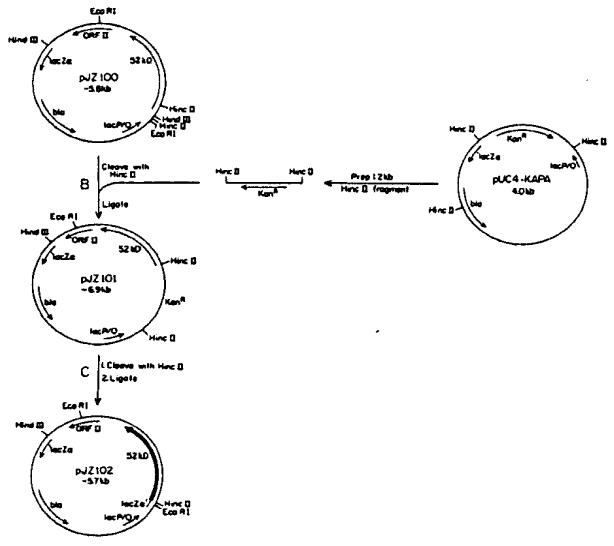

Fig. 10. Construction of an *hhc*$^{M}$-*lacZ* chimeric gene for bacterial expression of the 52-kD protein of *hhc*$^{M}$.

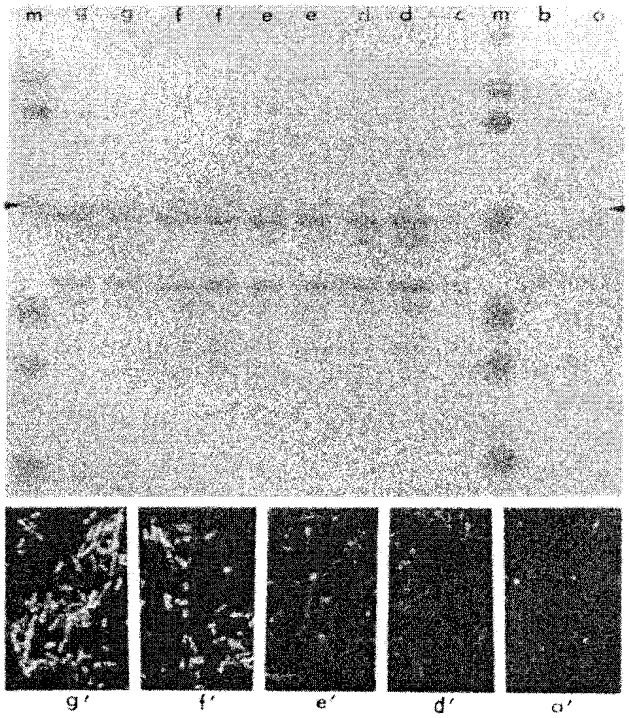

Fig. 11. Kinetic analysis of protein production in *E. coli* cells harboring pJZ102. Plasmid pJZ102 and control plasmid pJZ101 were cultured in *E. coli* cells until cell density reached a Klett reading of 80, at which point the inducer, IPTG (final concentration, $10^{-3}$ mol), was added to activate transcription from the *lac* promoter for the production of the chimeric *hhc*$^{M}$-*lac* 52-kD protein. One-ml samples of the cultures were removed at specified times, pelleted by centrifugation, lysed, and the proteins were denatured by boiling in Laemmli buffer. Equivalent aliquots of each sample were applied and analyzed by SDS-polyacrylamide gel electrophoresis as described elsewhere (25). *a*, pJZ102 + ITPG; *b*, pJZ102 − ITPG; pJZ102 + ITPG at 30 min (*d*), 4 h (*e*), 7 h (*f*), and 20 h (*g*). Dark field microscopy of pJZ102-transformed *E. coli* cells + ITPG at 0 time (*a'*), 30 min (*d'*), 4 h (*e'*), 7 h (*f'*), and 20 h (*g'*). Prestained molecular weight markers (*m*) in kD are 130 (*faint band on top*), 94, 75, 50, 39, 27, and 17.

## Discussion

Multiple attempts to transform liver cells with either DNA tumor viruses or by transfection with DNA from DNA tumor viruses have been reported. It was established earlier that hepatocytes could be immortalized by the transforming genes of either SV40 or polyoma virus (18–20). Cultured liver cells from transgenic mice carrying SV40 sequences demonstrated increased autonomy in growth and an independence from growth factor or hormone requirements (19). Similarly, neonatal rat hepatocytes, transfected with the plasmid pSV 5-neo carrying the polyoma virus early region after growth in various selective conditions including exposure to media containing growth factor and insulin, eventually became tumorigenic in nude mice. These cells were capable of secreting their own β-transforming growth factor-like activity (19). Certain rat hepatocyte lines harboring SV40 DNA became tumorigenic as they reached high passages in tissue culture (33 to 61) (11), a phenomenon of *in vitro* selection. The development of tumorigenicity in these cell lines was concomitant with increased expression of c-Ha-*ras*.

Neoplastic transformation of rat liver cells by transfection with a human DNA sequence, *hhc*$^{M}$, reported herein for the first time, was facilitated by the use of a neomycin resistance marker carried in the pNeo$^{r}$/S promoter vector. This vector contains an SV40 promoter sequence, a retroviral long terminal repeat, a partial T-antigen sequence, and a neomycin resistance gene. Transfection with this vector alone did not cause the typical cell transformation in BRL-1 cells nor did the transformants form tumors in either *nu/nu* mice or nude rats. BRL-1 and NIH3T3 cells transformed by pN$^{r}$pM-1 DNA showed morphological changes, such as an increase in refractility and loss of contact inhibition, and developed round and spindle-

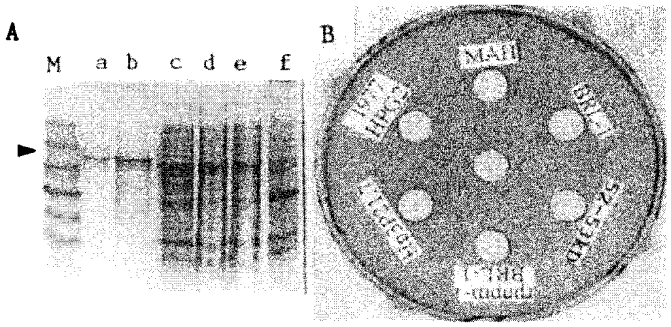


Fig. 12. *A*, purified *hhc*$^{M}$ fusion p52 produced in bacteria; *B*, specificity of a polyclonal anti-p52 immunoglobulin G. *A*, SDS-polyacrylamide gel electrophoresis of bacterially expressed p52. All conditions for the bacterial expression of chimeric *hhc*$^{M}$-*lac* fusion protein were as described in Fig. 11. *Lanes c* to *e* represent total cell extracts of pJZ102-bearing *E. coli* cells (in varying amounts) induced by IPTG, and *Lane f* represents the total cell extracts of a negative control pJZ101-bearing *E. coli* cells. *Lanes a* (5 μl) and *b* (15 μl) depict different amounts of gel-purified p52 that was used to immunize rabbits. *Lane M* depicts prestained molecular weight markers in kD (*i.l.*, 75, 57, 50, 39, 27, and 17). *Arrow*, purified 52-kD protein. *B*, reactivity of a polyclonal anti-p52. Anti-p52 polyclonal immunoglobulin was raised by immunizing rabbits. SDS-polyacrylamide gel-purified p52 at 0.8 to 1.0 mg each was used to immunize the New Zealand White rabbit by standard techniques. Two booster injections were given. Detergent (0.2% SDS)-lysed samples corresponding to 0.2 ml of packed human hepatoma cells (1/3; v/v) including Mahlavu hepatocellular carcinoma, Hp3p21.7 and HPG2, and pN$^{r}$pM-1-transfected BRL-1 tumor cells, control BRL-1 cells, and p52, at 10 μl each, were applied to the sample well and allowed to diffuse and cross-react overnight against the polyclonal anti-p52 immunoglobulin. Results were recorded at 48 h.

shaped cells, growth at high density with a tendency to detach, and anchorage-independent growth. Cells from transformed foci upon expansion (*i.e.*, at low passage) were tumorigenic in both Swiss-*nu/nu* mice and nude rats.

NIH3T3 cells transfected with DNAs from all three clones developed tumors in *nu/nu* mice, albeit with different latency periods. Tumor DNA samples contained *hhc*$^{M}$ sequences, yet the expression of neomycin resistance as well as anchorage-independent growth seemed to be independently regulated. Only one construct, pN$^{r}$pM-1, imparted stable characteristics of neomycin resistance, anchorage-independent growth, and tumorigenicity to transfected cells that persisted through successive tumor passages in nude mice. The inability of transformants derived from pN$^{r}$M and pN$^{r}$pM-2 DNAs to survive G418 selection and form colonies in soft agar was attributed to the cryptic expression of the neomycin resistance phenotype or abortive transformation, probably because of the orientation of the molecular constructs.

The characteristics of the transformed BRL-1 cells and NIH3T3 cells that incorporated pN$^{r}$pM-1 DNA confirmed that *hhc*$^{M}$ is a cell-transforming DNA. Morphologically, the primary BRL-1 transformants were of both epithelioid and glandular types. Following passage through *nu/nu* mice by either s.c. or i.p. inoculations, tumors that developed from BRL-1 transformants appeared histopathologically as both sarcomas and undifferentiated carcinomas. This suggests that the BRL-1 transformants that survived both G418 selection and animal passage were probably derived from the hepatic stroma or sinusoid. Sarcomas that developed from transformed hepatocytes have previously been observed among guinea pig hepatocytes transformed with UV-irradiated cytomegalovirus (21) and also in aflatoxin $B_1$-transformed rat hepatocytes (22).

Tumors produced in nude rats from the BRL-1 transformants were not as well defined in their histopathology. Certain tumors presented a histopathology characteristic of sarcoma, but there were also tumor masses that resembled minimally differentiated carcinoma. In this respect, tumors produced by BRL-1 cells transformed by pN$^{r}$pM-1 in nude rats resembled those that arose from rat hepatocytes (RL-PR-C) transformed by exposure to aflatoxin $B_1$. Tumors in the latter study were reportedly both sarcoma and carcinoma, demonstrating the multipotency of these epithelial cells transformed *in vitro* (22). It is of interest to note that *hhc*$^{M}$, the human transforming sequence, originated from an African (Mahlavu) hepatocellular carcinoma, the DNA of which showed high affinity for aflatoxin $B_1$ (6).

The multipotential nature of hepatocytes has also been explored in rats and hamsters (23, 24). The differentiation commitment of a rat hepatocyte could be reversed by subjecting the rat to a copper-deficient diet. This dietary manipulation depleted the pancreatic acinar cells almost completely and induced an infiltration of liver hepatocytes into 60% of the pancreas upon restoration to a normal diet. Morphological and histochemical evidence, as well as nucleic acid hybridization results, suggested that both ductular cells and interstitial cells, which resemble oval cells of the liver, may be considered equivalent to stem cells and are capable of undergoing transformation into pancreatic hepatocytes. In view of the versatility and multipotential nature of hepatocytes, cell transformation might not necessarily require a stem cell as target. A differentiated hepatocyte could be the target for cell transformation by *hhc*$^{M}$ DNA carried in pN$^{r}$pM-1, as shown here in terms of tumorigenic potential.

In this paper, we have also shown that *hhc*$^{M}$ encodes a 52-kD protein, and we have demonstrated that this DNA sequence can be readily expressed in bacteria. Earlier we found *hhc*$^{M}$-related DNA sequences in 19 hepatomas of Asian origin. Such DNA sequences were present in an amplified state which may have accounted for their detectability in these hepatomas (8). The amplification of cellular genes and/or certain protooncogenes and the elevated expression of certain proteins occur during liver regeneration, embryogenesis, or tumorigenesis. It would be of interest to investigate the expression of *hhc*$^{M}$-related p52 in patients at various stages of hepatocellular carcinoma and to compare such patients' specimens with samples from individuals suffering from liver cirrhosis, as well as other nonmalignant pathological conditions of the liver, such as hepatitis B or non-a non-b virus infections. Our results suggest that p52 and the specific polyclonal antiserum (anti-p52) offer possible screening and diagnostic applicability in areas of the world with populations at high risk of developing hepatocellular carcinoma, such as Africa, Japan, Taiwan, China, Korea, Thailand, India, Malaysia, and certain Mediterranean cities.

## Acknowledgments

The authors wish to acknowledge W. Vass, N. Basi, and R. Modali for their technical assistance.

## References

1. Blair, D. G., Oskarsson, M., Wood, T. G., McClements, W. C., Fischinger, P. J., and van de Woude, G. G. Activation of the transforming potential of a normal cell sequence: a molecular model for oncogenesis. Science (Wash. DC), *212:* 941–943, 1981.
2. Perucho, M., Goldfarb, M., Shimizu, K., Lama, C. Fogh, J., and Wigler, M. Human tumour-derived cell lines contain common and different transforming genes. Cell, *27:* 467–476, 1981.
3. Pulciani, S., Santos, E., Lauver, A. V., Long, L. K. Aaronson, S. A., and Barbacid, M. Oncogenes in solid human tumours. Nature (Lond.), *300:* 539–542, 1982.
4. Murray, M. J., Shilo, B-Z., Shih, T., Cowing, D., Hsu, H. W., and Weinberg, R. A. Three different human tumour cell lines contain different oncogenes. Cell, *25:* 355–361, 1981.

5. Weinberg, R. E. *ras* oncogenes and the molecular mechanisms of carcinogenesis. Blood, *64:* 1143–1145, 1985.
6. Yang, S. S., Taub, J., Modali, R., Vieira, W., Yasei, P., and Yang, G. C. Dose dependency of aflatoxin $B_1$ binding on human high molecular weight DNA in the activation of protooncogene. Environ. Health Perspect., *62:* 231–238, 1985.
7. Modali, R., and Yang, S. S. Specificity of aflatoxin binding on human protooncogene nucleotide sequence. M. Sorso and H. Norppa (eds), Prog. Clin. Biol. Res., *207:* 147–158, 1986.
8. Yang, S. S., Modali, R., Parks, J-B., and Taub, J. Transforming DNA sequences of human hepatocellular carcinomas, their distribution, and relationship with hepatitis B virus sequence in human hepatomas. Leukemia, *2:* 102s–113s, 1988.
9. Coon, H. G. 1968. Carnegie Inst. Wash. Year Book, *67:* 419–421, 1973.
10. Woodworth, C. D., and Isom, H. C. Transformation of differentiated rat hepatocytes with adenovirus and adenovirus DNA. J. Virol., *61:* 3570–3579, 1987.
11. Woodworth, C. D., Kreider, J. W., Mengel, L., Miller, T., and Isom, H. C. Tumorigenicity of simian virus 40-hepatocyte cell lines: effect of *in vitro* and *in vivo* passage on expression of liver-specific genes and oncogenes. Mol. Cell. Biol., *8:* 4492–4501, 1988.
12. Miller, E. C., and Miller, J. A. Mechanisms of chemical carcinogenesis. Cancer (Phila.), *27:* 2327–2345, 1981.
13. Graham, F. L., and Van der Eb, A. J. A new technique on the assay of infectivity of human adenovirus 5 DNA. Virology, *52:* 456–467, 1973.
14. Maniatis, T., Fritsch, E. F., and Sambrook, J. Molecular Cloning. Cold Spring Harbor, NY: Cold Spring Harbor Laboratory, 1982.
15. Yang, S. S., Modali, R., Wu, R., and Gardner, M. Molecular cloning of the endogenous rat C-type helper virus DNA sequence structural organization and functional analysis of some restricted DNA fragments. J. Gen. Virol., *63:* 25–36, 1982.
16. McKnight, S. L., and Kingsbury, R. Transcriptional control signals of a eukaryotic protein coding gene. Science (Wash. DC), *217:* 316–324, 1982.
17. Maxam, A. M., and Gilbert, W. Methods Enzymol., *65:* 499–506, 1980.
18. Isom, H. C., and Georgoff, I. Quantitative assay for albumin producing liver cells after simian virus 40 transformation of rat hepatocytes maintained in chemically defined medium. Proc. Natl. Acad. Sci. USA, *81:* 6378–6382, 1984.
19. Paul, D., Hohne, M., and Hoffmann, B. Immortalization and malignant transformation of hepatocytes by transforming genes of polyoma virus and of SV40 virus *in vitro* and *in vivo.* Klin. Wochenschr., *66:* Suppl. 11): 134–139, 1988.
20. Hohne, M., Piasecki, A., Ummelmann, E., and Paul, D. Transformation of differentiated neonatal rat hepatocytes in primary culture by polyoma virus early region sequences. Oncogene, *1:* 337–345, 1987.
21. Isom, H. C., Mummaw, J., and Kreider, J. W. Malignant transformation of guinea pig cells after exposure to ultraviolet-irradiated guinea pig cytomegalovirus. Virology, *126:* 693–700, 1983.
22. Schaeffer, W. I., and Heintz, N. H. A diploid rat liver cell culture. IV. Malignant transformation by aflatoxin $B_2$. In Vitro, *14:* 418–427, 1978.
23. Rao, M. S., Dwivedi, R. S., Yeldandi, A. V., and Subbarao, V. Role of periductal and ductular epithelial cells of the adult rat pancreas in pancreatic hepatocyte lineage. A change in the differentiation commitment. Am. J. Pathol., *134:* 1069–1086, 1989.
24. Rao, M. S., Subbarao, V., and Scarpelli, D. G. Development of hepatocytes in the pancreas of hamsters treated with 2,3,7,8-tetrachlorodibenzo-*p*-dioxin. J. Toxicol. Environ. Health, *25:* 201–205, 1988.
25. Somerville, R. L., Zeilstra-Ryalls, J. H., and Shieh, T-L. A general approach to defining the specificity of interactions between cytoplasmic proteins. *In:* P. Srere, M. E. Jones, and C. Mathews (eds.), Structural and Organizational Aspects of Metabolic Regulation: UCLA Symposia on Molecular and Cellular Biology, New Series, Vol. 133, pp. 181–197. New York: Alan R. Liss, Inc., 1990.